Reconfigurable microstrip patch antenna using gold and graphene material for high frequency communication.

Nizam Bilakhiya [1], Shobhit K. Patel [1, 2, *,] Vishal Sorathitya [1]

[1]Department of Electronics and Communication Engineering, Marwadi Education Foundation Group of Institutions, Gujarat, Rajkot, 360002 India

[2] Department of Electrical and Computer Engineering, University of Nebraska-Lincoln, Lincoln, NE, 68588, USA

[*] Corresponding author: shobhitkumar.patel@marwadieducation.edu.in, nizambilakhiya@gmail.com, vishal.sorathiya@marwadieducation.edu.in

Abstract - Recent advancement in antenna technology is directed to achieve reconfiguration in antenna parameters. The microstrip patch antenna can be designed to produce a variety of different parameters, like radiation pattern, reflection coefficient, Voltage Standing Wave Ratio. It depends on shapes which can have a dual or multi-frequency operation. Graphene got a lot of attention for its potential use in high-frequency applications due to its tunability property. By varying the chemical potential of graphene its material properties can be altered which results in tunable frequency response and reconfiguration can be achieved. In this paper, we have designed a graphene-based reconfigurable microstrip patch antenna for high-speed communication and multi-band application. The circular sheet of graphene as a radiating patch would be analyzed to study its radiating characteristics. By varying the chemical potential of graphene reconfigurable characteristics of the antenna have achieved. The performance of the graphene-based patch antenna in terms of its reflection coefficient, gain and radiation pattern have obtained.

Keywords: Microstrip patch antenna, Frequency band tuning, Split ring resonator, THz communication, Graphene antenna.

1. Introduction

For maximization of connectivity, requires the integration of multiple radios into a single platform which results in the advancement in wireless communications. Contrary to this, the Antenna plays an important role in the operation of all communication devices. Antenna, also known as a transducer, can transmit as well as receive signals, converts electrical signals to electromagnetic signals or vice-versa [1]. For the THz frequency range, various applications in enormous fields like imaging, sensing, quality control, wireless communication, and basic science can be utilized [2]. Antenna can be designed in many ways and their types are many based on different applications like to increase channel capacity MIMO systems are utilized [3], microstrip antennas can be used for THz range devices which can be suitable for different conditions[4], Reconfigurable antennas can deliver the same throughput as a multi-antenna system and vice versa. The antenna, being an integral part of many wireless devices, plays an important role in defining the performance of many of these devices. So for guaranteed good system-level performance, their design should be carried out with care. Among various kinds of antennas, printed antennas have received considerable attention during the past few decades as of their low-profile nature and their ease of integration with associated electronics, which make them very suitable in compact wireless devices [5]. These type of antennas have widely used in satellite communications, aerospace and radars. its inherent characteristics mechanically robust, compatible with integrated circuits and versatile resonant frequency, polarization, pattern, and impedance. Designs in shape of rectangular, circular, triangular for patch have been proposed in many research papers. A circular rectangular patch microstrip antenna is designed which increases the bandwidth [6]. For application in the medical field, rectangular shaped microstrip patch antenna [7] and an ultra-wideband (UWB) multi-resonant optical antenna [8] have been designed using FR4 substrate [9]. A novel microstrip patch antenna has been proposed and presented in [10].

Graphene was first demonstrated by Andre Geim and Konstantin Novoselov, from the University of Manchester, in 2004 [11-12]. Graphene is a promising material because of its excellent properties like electromagnetism and electromechanical, electrical conductivity [13-14]. Tunable characteristics can be observed by adjusting the chemical potential through bias voltage in graphene-based patch antennas, which is desirable highly for electromagnetic applications for THz frequencies. [15-16]. Based on typical properties, graphene can be utilized for wireless communication, which leads to interesting features such as

miniaturization, integration with graphene RF active electronics [17]. The designing and radiation characteristics of a graphene nanoribbon (GNR) based microstrip patch antenna on the polyimide substrate in the terahertz band is studied [18]. The researcher has designed a graphene-based patch antenna on the polyimide (εr = 3.5) substrate and investigated radiation characteristics of a graphene nanoribbon (GNR) based microstrip patch antenna in terahertz band [19]. A comparison of the radiation pattern of a graphene-based nano-patch antenna to that of an equivalent metallic antenna is studied [20].

In this paper, we focus on frequency reconfigurable graphene-based patch antenna which will be useful for high-speed communication. Two dielectric substrates are being used to mount graphene. A split ring resonator of gold material is also mounted along with graphene layer as microstrip patch. In this structure, two layers of graphene are being laid and observation is made, basis on changing the chemical potential of graphene. Normalized VSWR have been analyzed, tunability of frequency has been observed. Good reflection coefficient and gain are achieved.

2. Graphene Antenna Design:

2.1 Patch Antenna Design Considerations:

In this section, we present the proposed design of the graphene-based antenna. It's 3D representation can be shown as in Figure 1. The various parameters used for designing antenna are specified in Table 1. The antenna's length and width are denoted as L and W respectively, measured to as 60 μm. The ground layer is composed of copper material with a height of 6 μm as shown in Figure 1. Two substrates of FR4 material of height 4 μm is placed above the copper ground. The length and width of the ground and both substrates are considered to be the same as that of antenna's L and W. The first layer of graphene is laid between these two substrates. The second layer of graphene, circular in shape is placed above the second layer of FR4 substrate as shown in Figure 1. Above this circular graphene sheet, a gold split ring of radius 28 μm is mounted with the thickness of 10 μm denoted as d, and height as c = 2 μm. The thickness of graphene is considered to be 0.34nm. The dielectric constant (ε_r) of the FR4 substrate is taken to be 4.4.

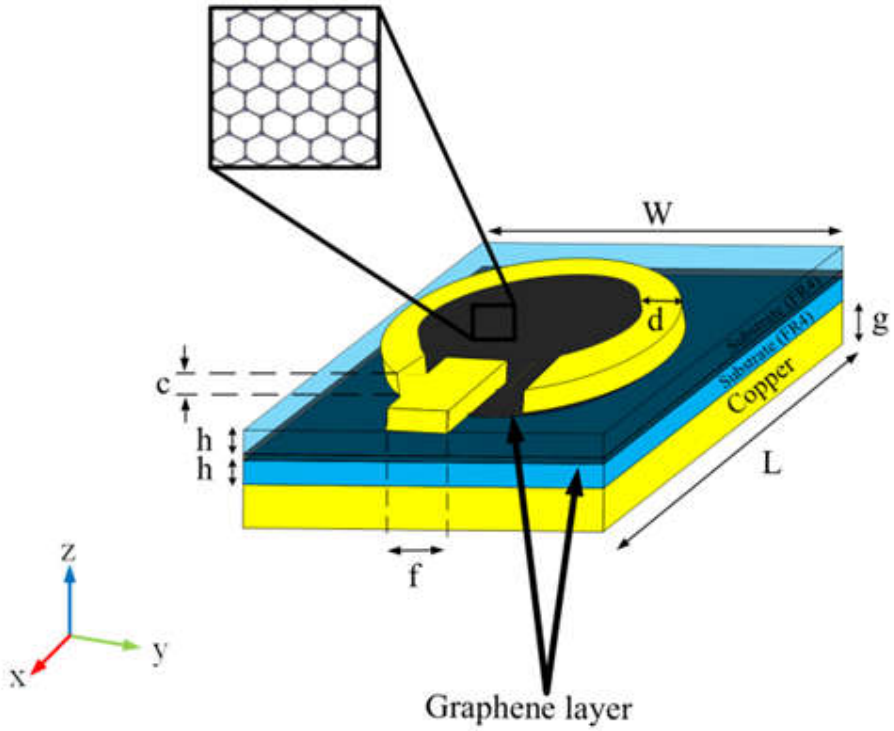

Figure: 1 Detailed 3D graphical representation of antenna. Antenna length and width denoted with L and W is 60 μm, Height of ground plane of copper denoted with g is 6 μm with same length width. Radius of split ring is 28 μm from centre of antenna, width of split ring denoted with d is 10 μm, height of split ring denoted as c is 2 μm, and same height of feed line. Width and length of feed line are 20 μm. Feed line denoted with f in figure. There are two Graphene layer taken, one place between two substrates with same length width of antenna, and second under the split ring in circular shape with radius of 28 μm. Substrate height denoted with h is 4 μm with same length width.

The relative permeability and permittivity of gold are taken from [21]. Figure 2 shows the 2D representation of the design where the grey colored space resembles a graphene layer and external biasing is given to these. To excite this antenna, a microstrip feeding technique with a center feed of width and length 20 μm is employed; height is same as the height of split ring. Figure 3 resembles the equivalent circuit of the antenna. The design is simulated using finite element method.

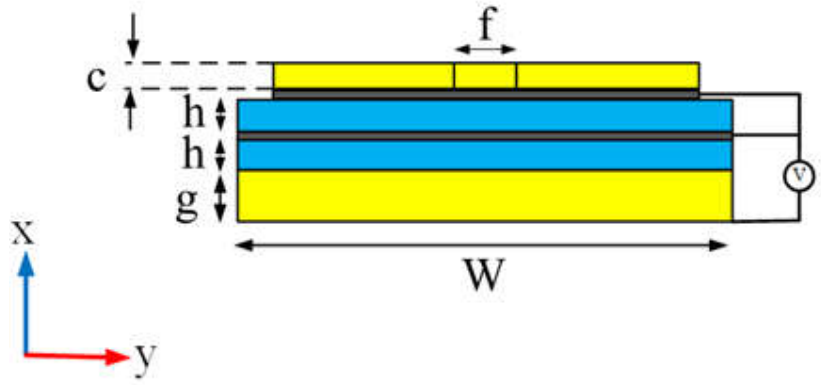

Figure: 2 2D Geometry of antenna. With applied external biasing (μ_c) chemical potential to the graphene layer. Ground height denoted with g, substrate height denoted with h, c represents height of gold split ring and feed line, f represents the feed line.

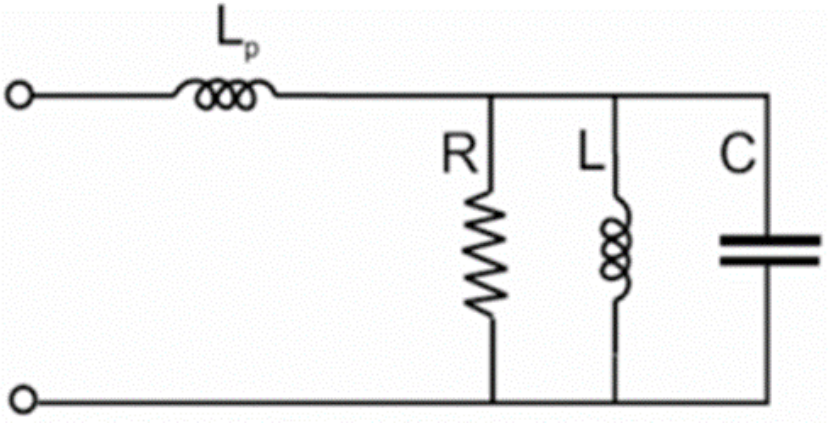

Figure: 3 Equivalent circuit of microstrip antenna.

2.2 Graphene conductivity model

The surface conductivity of graphene has been considered as the Kubo formula [22].

$$\sigma(\omega, \mu_c, \Gamma, T) = \frac{je^2(\omega - j2\Gamma)}{\pi\hbar^2}\left[\frac{1}{(\omega - j2\Gamma)^2}\int_0^\infty \varepsilon\left(\frac{\partial f_d(\varepsilon)}{\partial\varepsilon} - \frac{\partial f_d(-\varepsilon)}{\partial\varepsilon}\right)d\varepsilon - \int_0^\infty \frac{f_d(-\varepsilon) - f_d(\varepsilon)}{(\omega - j2\Gamma)^2 - 4(\varepsilon/\hbar)^2}d\varepsilon\right], \quad (1)$$

Where $f_d(\varepsilon) = \left(e^{(\omega-\mu_c)/k_BT} + 1\right)^{-1}$ is the Fermi-Dirac distribution where k_B is Boltzmann's constant, first term is due to intraband contributions, and the second term due to interband contributions, electron charge is represented as e, ω is radian frequency, μ_c is a chemical potential, Γ is a phenomenological scattering rate that is assumed to be independent of energy ε, T is temperature and $\hbar$ is the reduced Planck's constant. [22].

3. Results and discussion

In this section, we are studying various parameters of an antenna. One of the key performance indicators for an antenna is the reflection coefficient (S11 parameter). For resonant frequencies, a sufficient reflection coefficient is achieved. Figure 4 represents the reflection coefficient versus resonant frequency of the antenna. It is observed that the reflection coefficient is shifting (tune) at a different frequency range by changing the chemical potential μ_c (eV) of graphene. It is evident from figure 4, that there is a shifting of the reflection coefficient at a different frequency with respect to different applied chemical potential μ_c (eV). The proposed graphene antenna represent the tunability over the frequency range of 1.33 THz to 1.35 THz. We have explored the results of the graphene-based antenna by changing chemical potential μ_c (eV).

We can see that in figure 4, when the chemical potential μ_c 0.08 eV is applied, the reflection coefficient is reaching about -46.52 dB at 1.34 THz frequency. It is among the better reflection coefficient achieved than other applied chemical potential, with achieved gain of 4.85 dB. For other chemical potential μ_c, reflection coefficient value lesser than -10 dB have been observed. When chemical potential μ_c 0.04 eV is applied, the reflection coefficient is -41.6 dB at 1.33 THz frequency with achieved gain of 4.24 dB. And when chemical potential μ_c 0.11 eV is applied, the reflection coefficient is -34.27 dB at 1.35 THz frequency with achieved gain of 5.3 dB. In figure 4, the blue line indicates the reflection coefficient for μ_c 0.04 eV, the red line indicates the reflection coefficient for μ_c 0.08 eV and the black line indicate the reflection coefficient for μ_c 0.11 eV.

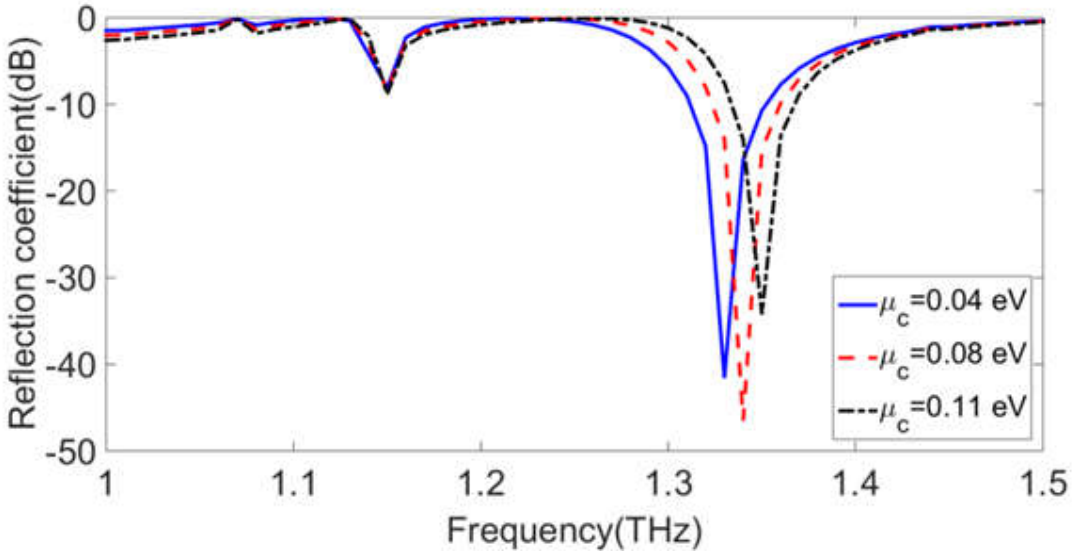

Figure: 4 Reflection coefficient versus frequency of antenna for different applied chemical potential. Reflection coefficient shift (tune) at different frequency range, it is achieved by changing the chemical potential (μ_c) of graphene. (Blue line represent 0.04 eV, red line represent 0.08 eV and black line represent 0.11 eV)

Voltage Standing Wave Ratio (VSWR), is the ratio of a maximum voltage amplitude of a standing wave to the minimum voltage amplitude. It is considered as one of the key parameter of the antenna. The value of VSWR nearer to 1 is considered to behave as a good antenna matching. Figure 5 represents the Voltage Standing Wave Ratio of the antenna at different applied chemical potential. The blue line indicates VSWR for μ_c 0.04 eV, the red line indicates VSWR for μ_c 0.08 eV and green line indicate VSWR for μc 0.11 eV. The resonance frequency ranges from 1.33 THz to 1.35 THz. At all these frequencies, the value of VSWR is achieved to be 1.

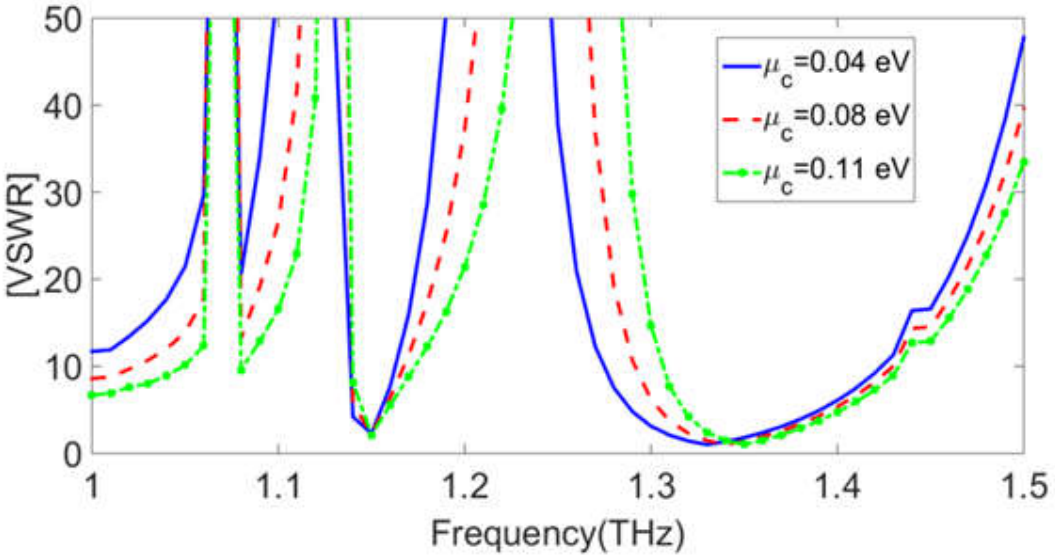

Figure: 5 Voltage Standing Wave Ratio of antenna at different applied chemical potential. (Blue line represent 0.04 eV, red line represent 0.08 eV and green line represent 0.11 eV)

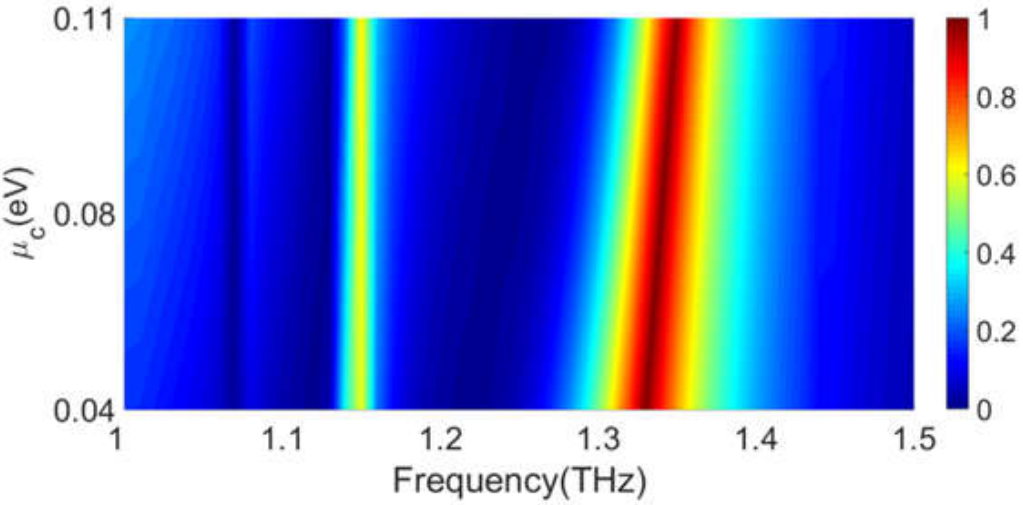

Figure: 6 Reflection coefficient response at different chemical potential (μ_c) for 1 THz to 1.5 THz frequency range. Colour bar indicates normalized reflection coefficient. Blue colour corresponds to minimum reflection coefficient and red colour indicates maximum reflection coefficient.

Figure 6 indicates the reflection coefficient response for the different chemical potential (μ_c) between 1 THz to 1.5 THz frequency range. Right side colour bar indicates the normalized reflection coefficient. Blue colour corresponds to minimum reflection coefficient and red colour indicates maximum reflection coefficient. We can clearly see the shifting of reflection coefficient band from 1.33 THz to 1.35 THz, with respect to the changing of chemical potential μ_c from 0.04 eV to 0.11 eV respectively.

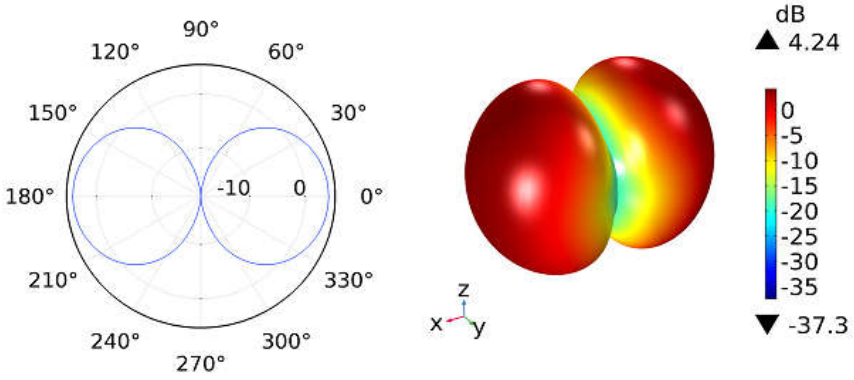

Figure: 7 [A] Far field 2D polar plot and **[B]** Far field 3D radiation pattern at μc 0.04 eV, frequency 1.33 THz with achieved gain of 4.24 dB.

Figure 7 [A] represents the far-field 2D Polar plot and figure 7 [B] represent Far field 3D Radiation pattern of the antenna for applied chemical potential μ_c 0.04 eV at frequency 1.33 THz with achieved Gain of 4.24 dB. Figure 8 [A] represents the far-field 2D Polar plot and Figure 8 [B] represent Far field 3D Radiation pattern of the antenna for applied chemical potential μ_c 0.08 eV at frequency 1.34 THz with achieved Gain of 4.85 dB. Figure 9 [A] represents the far-field 2D Polar plot and Figure 9 [B] represent Far field 3D Radiation pattern of the antenna for applied chemical potential μ_c 0.11 eV at frequency 1.35 THz with achieved Gain of 5.3 dB. In all the Far-field, 3D Radiation pattern, the colour bar shows the

minimum and maximum value of gain of the antenna. The maximum gain of 5.3 dB is achieved for chemical potential μ_c 0.11 eV. The results of the reflection coefficient, gain and VSWR for changing chemical potential μ_c at the different resonant frequency is shown in table 2.

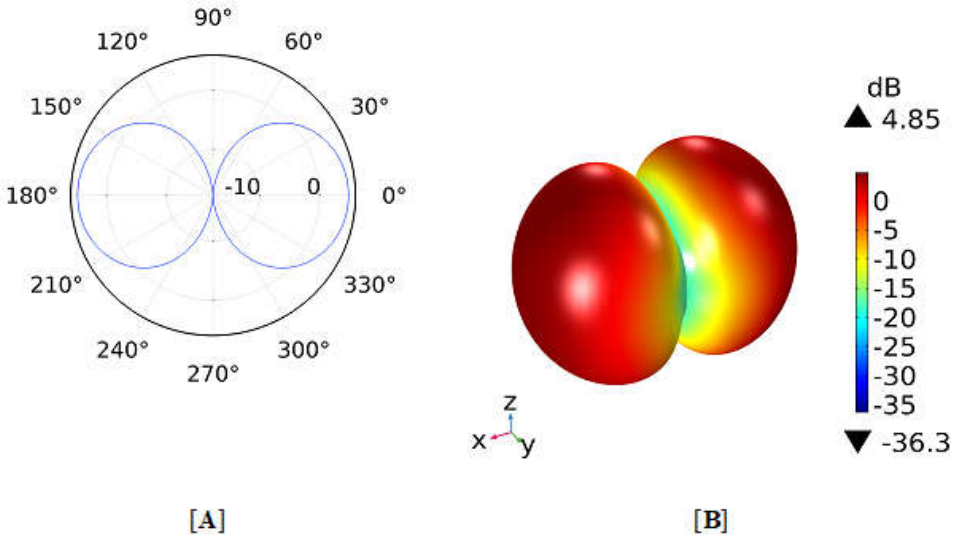

Figure: 8 [A] Far field 2D polar plot and **[B]** Far field

Measured bandwidth of 30 GHz is achieved at 1.33 THz frequency. 20 GHz bandwidth at 1.34 THz frequency and at this frequency reflection coefficient (s11) shift (tuning) of 10 GHz from the reference of 1.33 THz frequency for applied chemical potential μ_c 0.04 eV is achieved. 20 GHz bandwidth is achieved at 1.35 THz frequency and also reflection coefficient (s11) shift (tuning) of 10 GHz from the reference of 1.34 THz frequency for chemical potential μ_c 0.08 eV, is achieved. For reflection coefficient, bandwidth is measured less than – 10 dB. The detailed measured result for different parameters of the antenna is shown in table 2.The different electric field produced by the antenna with respect to applied different chemical potential μ_c (eV) is shown in Figure 10. Figure 10 [A] demonstrates the Electric field of the antenna at Frequency 1.33 THz, when the chemical potential μ_c 0.04 eV is applied. Figure 10 [B] demonstrates the Electric field of the antenna at Frequency 1.34 THz, when the chemical

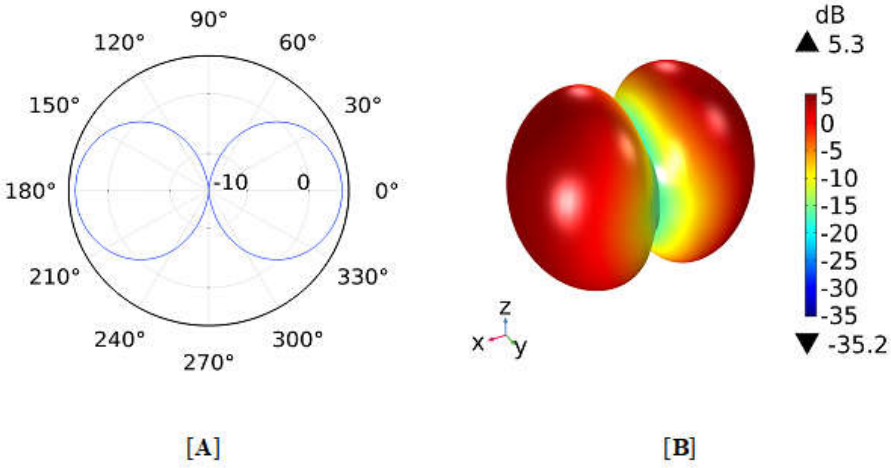

Figure: 9 [A] Far field 2D polar plot and **[B]** Far field 3D radiation pattern at μc 0.11 eV, frequency 1.35 THz with achieved gain of 5.3 dB.

potential μ_c 0.08 eV is applied. Figure 10 [C] demonstrates the Electric field of the antenna at Frequency 1.35 THz, when the chemical potential μ_c 0.11 eV is applied.

Table: 1 Parameters used in designing antenna.

	Parameters	**Values (μm)**
W	Substrate width	60
L	Substrate length	60
c	patch height	2
d	Width of split ring	10
f	Width of feed line	20
g	Height of ground	6
h	Height of substrate	4

Table: 2 Simulated measured result at different parameters of antenna.

No.	**μc (eV)**	**Resonant Frequency (THz)**	**Reflection coefficient (dB)**	**Gain (dB)**	**VSWR**	**Bandwidth (GHz) (S11 < -10 dB)**	**Frequency shifting (GHz) with reference μc (eV)**	
1	0.04	1.33	-41.6	4.24	1	30	(GHz)	(eV)
2	0.08	1.34	-46.52	4.85	1	20	10	0.04
3	0.11	1.35	-34.27	5.3	1	20	10	0.08

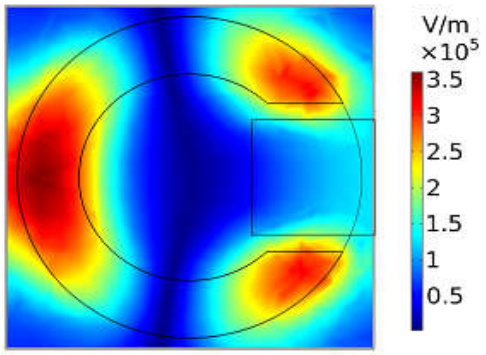

[A]

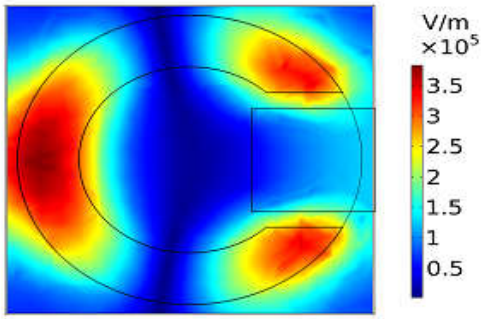

[B]

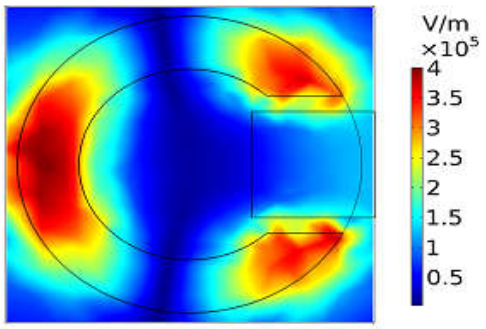

[C]

Figure: 10 [A] Electric field at μc 0.04 eV, frequency 1.33 THz. **[B]** Electric field at μc 0.08 eV, frequency 1.34 THz. **[C]** Electric field at μc 0.11 eV, frequency 1.35 THz.

4. Conclusion

The design, reflection coefficient and radiation characteristic of the graphene-based microstrip patch antenna for the terahertz frequency band is presented. In this novel approach of the graphene-based antenna, we observed that tunable frequency response is achieved with respect to different chemical potential. Good reflection coefficient, VSWR and gain are achieved. By increasing the chemical potential, gain is increased. The radiation pattern of the proposed antenna is shown in figure [7, 8, 9] and listed gain in table 2. By different analysis and observation, it can be concluded that the graphene-based microstrip antenna has the potential to be integrated into high-speed THz communication devices, and it can be used in the multiband application.

References

[1] Antenna Theory Analysis And Design 3rd Ed. By Constantine A. Balanis . JOHN WILEY & SONS, INC., PUBLICATION.

[2] Hafez, H. A., Chai, X., Ibrahim, A., Mondal, S., Férachou, D., Ropagnol, X., & Ozaki, T. (2016). Intense terahertz radiation and their applications. Journal of Optics, 18(9), 093004.

[3] Li, H., Xiong, J., & He, S. (2009). A compact planar MIMO antenna system of four elements with similar radiation characteristics and isolation structure. Antennas and Wireless Propagation Letters, 8, 1107-1110.

[4] R. Bala, A. Marwaha, Characterization of graphene for performance enhancement of patch antenna in THz region, Optik - Int. J. Light Electron Opt. (2015).

[5] Khan, M. U., Sharawi, M. S., & Mittra, R. (2015). Microstrip patch antenna miniaturisation techniques: a review. IET Microwaves, Antennas & Propagation, 9(9), 913-922.

[6] Gopal, E., & Singhal, A. (2018). Design & Simulation of Circular Rectangular Microstrip Patch Antenna for Wireless Applications.

[7] Kalra, P., & Sidhu, E. (2017, March). Rectangular TeraHertz microstrip patch antenna design for riboflavin detection applications. In Big Data Analytics and Computational Intelligence (ICBDAC), 2017 International Conference on (pp. 303-306). IEEE.

[8] Singh, V., Nag, A., & Sidhu, E. (2016, March). High gain ultra wide band (UWB) multi resonant antenna for biomedical applications, security purposes and drug detection. In Wireless Communications, Signal Processing and Networking (WiSPNET), International Conference on (pp. 927-930). IEEE.

[9] Patel, S. K., Shah, K. H., & Kosta, Y. P. (2018). Multilayer liquid metamaterial radome design for performance enhancement of microstrip patch antenna. *Microwave and Optical Technology Letters*, *60*(3), 600-605.

[10] Kushwaha, R. K., Karrupanan, P., & Malviya, L. D. (2018). Design and analysis of novel microstrip patch antenna on photonic crystal in THz. Physica B: Condensed Matter

[11] Novoselov, K. S., Geim, A. K., Morozov, S. V., Jiang, D. A., Zhang, Y., Dubonos, S. V., ... & Firsov, A. A. (2004). Electric field effect in atomically thin carbon films. science, 306(5696), 666-669.

[12] Goyal R, Vishwakarma DK. Design of a graphene-based patch antenna on glass substrate for high-speed terahertz communications. Microw Opt Technol Lett. 2018;60:1594–1600.

[13] Marinho, B., Ghislandi, M., Tkalya, E., Koning, C. E., & de With, G. (2012). Electrical conductivity of compacts of graphene, multi-wall carbon nanotubes, carbon black, and graphite powder. Powder Technology, 221, 351-358.

[14] Ziegler, K. (2007). Minimal conductivity of graphene: Nonuniversal values from the Kubo formula. Physical Review B, 75(23), 233407.

[15] Dave, V., Sorathiya, V., Guo, T., & Patel, S. K. (2018). Graphene based tunable broadband far-infrared absorber. Superlattices and Microstructures, 124, 113-120.

[16] Thomas, L., Sorathiya, V., Patel, S. K., & Guo, T. Graphene-based tunable near-infrared absorber. Microwave and Optical Technology Letters.

[17] Lin, Y.M., Jenkins, K.A., Valdes-Garcia, A., et al.: 'Operation of graphene transistors at gigahertz frequencies', Nano Lett., 2008, 9, (1), pp. 422–426, doi: 10.1021/nl803316h

[18] Anand, S., Sriram Kumar, D., Wu, R. J., & Chavali, M. (2014). Graphene nanoribbon based terahertz antenna on polyimide substrate. Optik - International Journal for Light and Electron Optics, 125(19), 5546–5549

[19] Rajni Bala, Anupma Marwaha, Investigation of graphene based miniaturized terahertz antenna for novel substrate materials, Engineering Science and Technology, an International Journal (2015), doi: 10.1016/j.jestch.2015.08.004

[20] Llatser, I., Kremers, C., Chigrin, D. N., Jornet, J. M., Lemme, M. C., Cabellos-Aparicio, A., & Alarcón, E. (2012, March). Characterization of graphene-based nano-antennas in the terahertz band. In Antennas and Propagation (EUCAP), 2012 6th European Conference on (pp. 194-198). IEEE.

[21] Ghosh, G. (1998). Handbook of optical constants of solids: Handbook of thermo-optic coefficients of optical materials with applications. Academic Press.

[22] Hanson, G. W. (2008). Dyadic Green's functions and guided surface waves for a surface conductivity model of graphene. *Journal of Applied Physics*, *103*(6), 064302.